RSC Advances

PAPER

View Article Online
View Journal | View Issue

Cite this: *RSC Adv.*, 2024, **14**, 22763

Hybridization of short-range and long-range charge transfer boosts room-temperature phosphorescence performance†

Tian-Miao Li,‡[ab] Li-Yuan Hu,‡[b] Xin Zou,*[c] Jun-Yi Wang,[b] Sheng Ni,[b] Lei Liu,*[a] Xunwen Xiao*[bd] and Xu-Feng Luo*[b]

Received 4th May 2024
Accepted 6th July 2024

DOI: 10.1039/d4ra03283g

rsc.li/rsc-advances

At present, mainstream room-temperature phosphorescence (RTP) emission relies on organic materials with long-range charge-transfer effects; therefore, exploring new forms of charge transfer to generate RTP is worth studying. In this work, indole-carbazole was used as the core to ensure the narrowband fluorescence emission of the material based on its characteristic short-range charge-transfer effect. In addition, halogenated carbazoles were introduced into the periphery to construct long-range charge transfer, resulting in VTCzNL-Cl and VTCzNL-Br. By encapsulating these phosphors into a robust host (TPP), two host–guest crystalline systems were further developed, achieving efficient RTP performance with phosphorescence quantum yields of 26% and phosphorescence lifetimes of 3.2 and 39.2 ms, respectively.

Introduction

Organic room-temperature phosphorescence (RTP) materials have shown promising applications in anti-counterfeiting, optical imaging, flexible displays, and solid-state lighting.[1–7] Different from inorganic and carbon-dot afterglow materials, organic RTP materials have become a research hotspot owing to their diverse structural designs and adjustable photophysical characteristics.[8–15] Currently, most reported organic RTP materials have been designed and synthesized by introducing a donor and acceptor to achieve a long-range charge-transfer effect for enhancing the intersystem crossing process, which is similar to the construction of traditional thermally activated delayed fluorescence (TADF) materials.[16–21] However, because of the molecular structural relaxation and vibrational coupling between the ground state (S_0) and the lowest singlet state (S_1), these materials exhibited full width at half maxima (FWHM) values exceeding 70 nm.[22,23] Therefore, proposing an approach to decrease the FWHM values of organic RTP materials is crucial for promoting their further application and development.

Organic materials with rigidity and short-range charge-transfer (SR-CT) effects have exhibited almost high fluorescence radiation rates, intersystem crossing rates (k_{ISC}), and narrow-emission spectra.[24–27] Following the aforementioned principles, multi-resonance frameworks (such as boron-nitrogen (B/N), carbonyl-nitrogen (C=O/N), and indolocarbazole (ICz)) were developed to obtain a series of narrowband MR-TADF materials with blue-to-red emissions.[28–33] To boost RTP performances, the k_{ISC} of emitters should be accelerated again. Notably, ICz-based MR materials exhibit a small FWHM, a large ΔE_{ST}, and a sole fluorescence emission. In recent reports, by reasonably designing a molecular framework, the long lifetimes of ICz-based materials could be regulated while maintaining their narrow-emission characteristics.[34] Therefore, organic integration of the ICz framework to achieve efficient RTP performance is a potential and direct means of constructing narrow-emission afterglow materials.

Herein, based on a push–pull electron effect, an ICz-type MR core was selected as the electron-withdrawing group, and carbazole derivatives as the electron-donating group were introduced on the periphery to achieve hybridization of SR-CT and LRCT.[35] In addition, the substitution of peripheral halogenated elements (Cl and Br atoms) of carbazole further contributed to the effective k_{ISC} through a heavy-atom effect. The single crystals of two molecules further confirmed the twisted conformation between ICz and halogenated carbazole, which could effectively suppress π–π stacking in the solid state and reduce energy dissipation through non-radiative decay

[a]*College of Chemical and Pharmaceutical Engineering, Hebei University of Science and Technology, Shijiazhuang 050018, China*

[b]*College of Material Science and Chemical Engineering, Ningbo University of Technology, Ningbo 315211, P. R. China*

[c]*Frontiers Science Center for Flexible Electronics (FSCFE), Northwestern Polytechnical University, Xi'an 710072, P. R. China*

[d]*State Key Laboratory of Applied Organic Chemistry (Lanzhou University), Lanzhou 730000, China*

† Electronic supplementary information (ESI) available: Experimental procedures, crystallographic data, structural data, spectroscopic data. CCDC 2338861 and 2338875. For ESI and crystallographic data in CIF or other electronic format see DOI: https://doi.org/10.1039/d4ra03283g

‡ These authors contributed equally to this work.

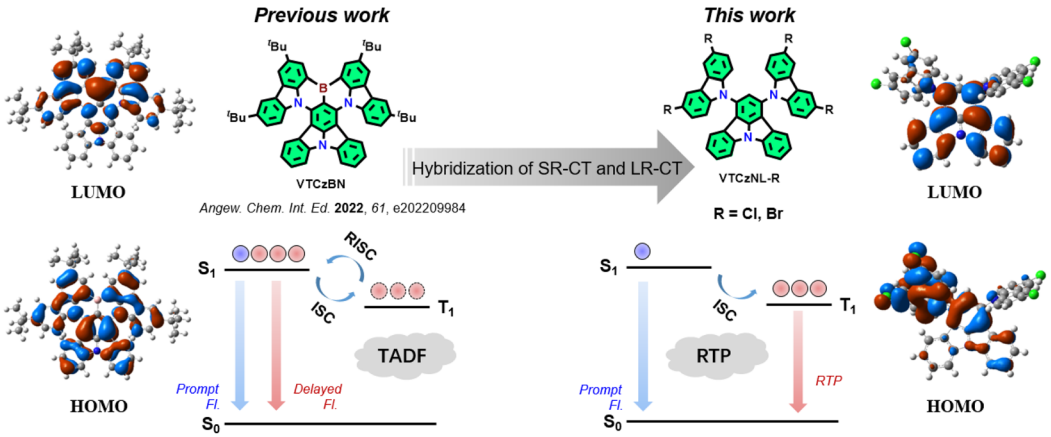

Fig. 1 Molecular design strategies and electron cloud distribution of the HOMO and LUMO for the case study of VTCzNL-Cl.

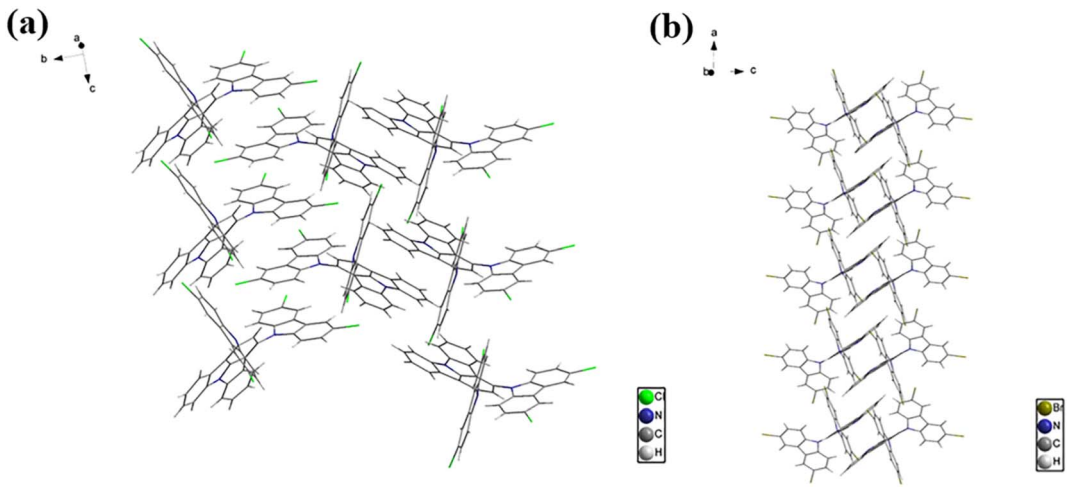

Fig. 2 (a) Crystal packing of VTCzNL-Cl. (b) Crystal packing of VTCzNL-Br showing H-aggregation.

channels. By encapsulating these afterglow materials into a host (TPP), two host–guest cocrystalline systems were further developed, showing narrowband emission peaking at 420 nm with a FWHM of ~40 nm, efficient RTP performances with a phosphorescence quantum efficiency (ϕ_P) of 26% and lifetimes (τ_P) of 3.2 and 39.2 ms (Fig. 1 and 2).

Results and discussion

Synthesis and characterization

The key intermediate ICzBF was synthesized according to the previous literature.[35] Subsequently, the target products VTCzNL-Cl and VTCzNL-Br were obtained by a classic nucleophilic substitution between chlorinated and brominated carbazole and the key intermediate ICzBF. Further, two molecular structures were validated through NMR and mass spectrometry. Thermogravimetric analysis (TGA) analysis was also applied and indicated that the two materials had good thermal stability (Fig. S11†).

Additionally, VTCzNL-Cl and VTCzNL-Br were slowly diffused in DMF to obtain respective crystals. Single-crystal structure analysis showed that the two molecules presented butterfly-shaped spatial configurations, and twist angles of 118.704° and 120.332° were observed between the carbazole derivatives and the ICz core. Due to the planar characteristics of the ICz core, both VTCzNL-Cl and VTCzNL-Br exhibited significant H-aggregation caused by the strong π–π interactions.[36–38] The weak intermolecular forces also contributed to the aggregation of adjacent molecules. For VTCzNL-Cl, a C–H···π distance of 2.841 Å was observed, which is beneficial for restricting molecular motion. For VTCzNL-Br, C–H···π distances of 2.820–2.896 were observed, which could not only stabilize multiple frameworks, but also suppress non-radiative transitions. Interestingly, the rigid combination of fragments facilitated by the planar ICz core and connected chlorinated and brominated carbazole units is beneficial for inducing a more rigid environment to minimize the non-radiative decay, providing an effective pathway for the utilization of triplet excitons through a radiative process. The above structural arrangement and configuration characteristics provided good support for the formation of H-aggregation, which could further stabilize the triplet excitons and provide a possibility for room-temperature phosphorescence emission.

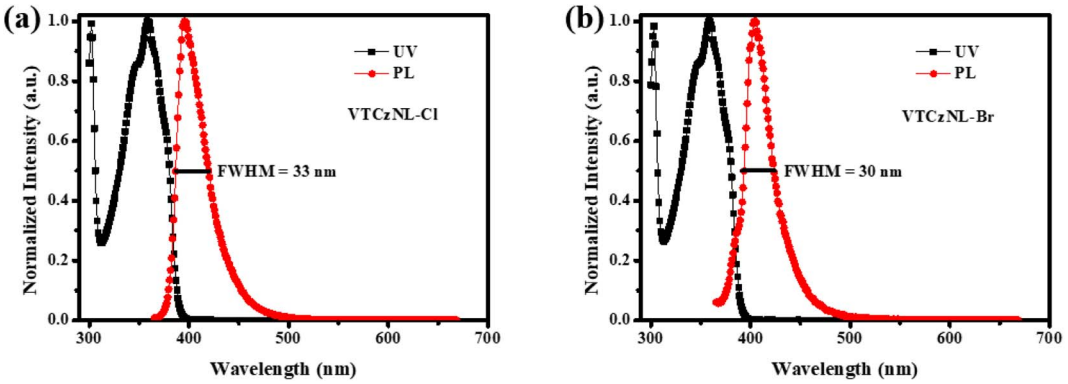

Fig. 3 UV-vis absorption and fluorescence emissions of VTCzNL-Cl (a) and VTCzNL-Br (b).

Table 1 Recorded photophysical properties of the two materials

Compounds	λ_{abs}[a] (nm)	λ_{em}[a] (nm)	FWHM[a] (nm)	S_1[b] (eV)	T_1[b] (eV)	ΔE_{ST}[c] (eV)
VTCzNL-Cl	358	396	33	3.04	2.58	0.46
VTCzNL-Br	358	404	30	3.02	2.61	0.41

[a] Measured at room temperature in toluene solution. [b] Measured at 77 K in toluene solution. [c] $\Delta E_{ST} = S_1 - T_1$.

The UV-vis absorption and fluorescence emissions of VTCzNL-Cl and VTCzNL-Br were characterized in toluene solution (Fig. 3), respectively. Intense and sharp absorption bands peaking at 358 nm for the two materials were observed, which were attributed to the molecular SR-CT features. Consistent with the emission characteristics of materials with a multiple resonance nature, the fluorescence emission spectra of the two materials exhibited a clear mirror relationship with the UV-vis absorption spectra, and small Stokes shifts were achieved. The fluorescence emissions of VTCzNL-Cl and VTCzNL-Br displayed peaks at 396 and 404 nm, with small FWHMs of 33 and 30 nm, respectively (Table 1).

To further determine the energy gap difference between the single and triplet states of the two materials, the fluorescence and phosphorescence spectra were obtained at 77 K. As illustrated in Fig. S6 and S7,† calculated from the emission peaks of fluorescence spectra at 77 K, the S_1 energies of VTCzNL-Cl and VTCzNL-Br were 3.04 and 3.02 eV, respectively. Also, estimated from the phosphorescence spectra at 77 K, the T_1 energies of VTCzNL-Cl and VTCzNL-Br were 2.58 and 2.61 eV, respectively. Based on the above calculation results for the S_1 and T_1 states energies, the ΔE_{ST} values of VTCzNL-Cl and VTCzNL-Br were estimated as 0.46 and 0.41 eV, respectively. The large ΔE_{ST} values are not conducive to achieving the upconversion behavior of T_1 excitons, which can effectively avoid the implementation of the TADF process. These two compounds exhibited only a long single exponential phosphorescence lifetime, whether in toluene solution or doped in TPP. (Fig. S11†). This is also a powerful experimental result to prove the absence of TADF.

In order to study the characteristics of the ground and excited states of the two molecules, density functional theory (DFT) calculations with the B3LYP/6-31g(d,p) basis set were carried out. The hybridization of the SR-CT and LR-CT was observed (Fig. 4). The SR-CT effect was implemented by the different electronegativity moieties (C and N atoms) within the ICz core, which was limited to the ICz core. Also, an LR-CT effect originated from a pull–push effect based on the carbazole derivatives with electron-donating abilities and the central ICz core with electron-withdrawing abilities. Due to the further introduction of the heavy atoms Cl and Br, the ISC process was improved, also enhancing the phosphorescence properties of the two materials, respectively. Additionally, the two materials exhibited similar highest occupied molecular orbital (HOMO) and lowest unoccupied molecular orbital (LUMO) energy levels, which was attributed to the basically consistent parent core framework, with the only difference being the substitution of Cl or Br atoms on the periphery. This also lays the foundation for comparing the performance of the halogenated elements in the final RTP performances of their host–guest systems.

To further stabilize the triplet excitons, the concept of host–guest doping is highlighted. Accordingly, the RTP performance of two materials could be further improved by means of the unique characters of the host. In this work, the rigid host molecule triphenylphosphine (TPP) was used and the method of melting the hosts and guests was chosen to better stabilize and utilize the triplet excitons of the guests. Two guests were doped with a 0.5% mass fraction in the hosts, as detected by HPLC (Fig. S8 and S9†). Also, the temperature for melting the host and guest molecules was 130 °C.

The two complexes exhibited deep-blue emissions at a steady state, while an apparently homogeneous green afterglow could be observed after ceasing illumination (Fig. 5c and f). Under 365 nm excitation, the guest material in the cocrystal systems

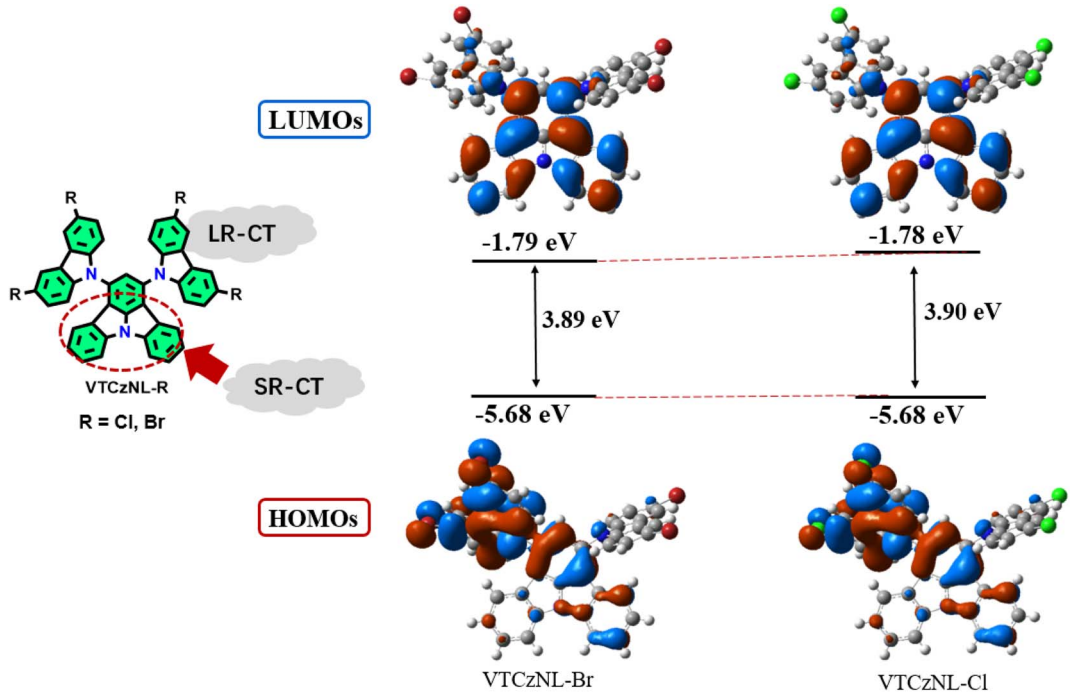

Fig. 4 HOMO and LUMO electron cloud distribution patterns.

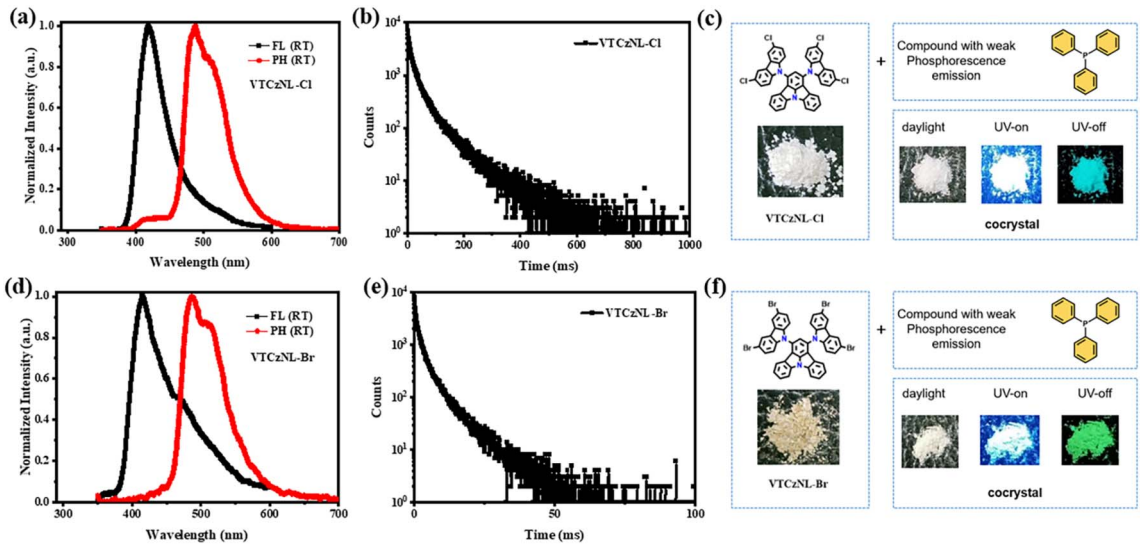

Fig. 5 (a) Room-temperature fluorescence and phosphorescence spectra of the VTCzNL-Cl-based complex. (b) Transient lifetime of the VTCzNL-Cl-based complex. (c) Cocrystal obtained by dissolving VTCzNL-Cl in the TPP host and photos taken of this before and after 365 nm UV lamp irradiation. (d) Room-temperature fluorescence and phosphorescence spectra of the VTCzNL-Br-based complex. (e) Transient lifetime of the VTCzNL-Br-based complex. (f) Cocrystal obtained by dissolving VTCzNL-Br in the TPP host and its photos taken before and after 365 nm UV lamp irradiation.

could only be excited, while the host material could not be excited. The two complexes showed deep-blue and narrowband fluorescence emissions peaking at 419 and 417 nm with FWHMs of 46 and 48 nm, respectively (Fig. 5a and d). After ceasing external excitation, the two complexes displayed green afterglow emissions (Fig. 5a and d) peaking at 488 and 489 nm, with FWHMs of 65 and 66 nm, respectively (Fig. 5a and d), which were narrower than those of most organic afterglow materials. Compared to the intrinsic fluorescence and phosphorescence emissions of TPP (Fig. S12†), the fluorescence and phosphorescence emissions of the two host–guest-doped complexes originated from the reported molecules in this work. According to the difference in the effect of increasing the heavy-atom effects on the SOC of materials, the complex based

on VTCzNL-Cl exhibited a longer phosphorescence lifetime (39.2 ms) than that (3.2 ms) of the complex based on VTCzNL-Br (Fig. 5b and e). The afterglow times of the VTCzNL-Cl-based and VTCzNL-Br-based complexes were 0.8 and 0.4 s, respectively (Fig. S10†). Benefiting from the rigid molecular skeletons, both complexes showed high phosphorescence quantum yields of 26%. The prolonged fluorescence may be further used for a background-free time-gated luminescence assay.[39]

Conclusions

In summary, VTCzNL-Cl and VTCzNL-Br with SR-CT and LR-CT characteristics were synthesized. Based on their rigid molecular skeletons, the two materials showed intense emission and suppressed non-radiative decay. The room-temperature phosphorescence based on the two host–guest systems showed long phosphorescence lifetimes of 3.2 and 39.2 ms and narrowband fluorescence and phosphorescence emissions. These results provide insights for guiding the design of narrow-emission afterglow materials.

Experimental

The synthesis routes of VTCzNL-Cl and VTCzNL-Br are shown in Fig. S1.† All the experiments were carried out under a nitrogen atmosphere. The raw materials and solvents were used as commercial grade without further purifications. The main ligands were synthesized by nucleophilic substitution.

Synthesis of VTCzNL-Cl

First, ICzBF (100 mg, 0.36 mmol), 3,6-dichloro-9*H*-carbazole (168 mg, 0.72 mmol), and Cs_2CO_3 (352 mg, 1.08 mmol) were dissolved in DMAC (20 ml) at room temperature. The mixture was stirred at 170 °C for 8 h. After cooling to room temperature, the reaction mixture was poured into a large amount of water. The product was extracted with dichloromethane and the combined organic layers were dried with anhydrous $MgSO_4$. Then, the crude product was evaporated, and recrystallized to obtain the white solid VTCzNL-Cl. (204 mg, yield: 80%). ^{1}H NMR (500 MHz, Chloroform-*d*) δ 8.15 (d, J = 1.7 Hz, 4H), 8.01 (d, J = 8.1 Hz, 2H), 7.77 (s, 1H), 7.59 (td, J = 7.8, 1.2 Hz, 2H), 7.44–7.31 (m, 8H), 7.19–7.11 (m, 2H), 6.97 (d, J = 7.8 Hz, 2H). ^{13}C NMR (126 MHz, Chloroform-d) δ 138.43, 138.29, 128.93, 126.87, 126.43, 126.11, 125.57, 124.37, 122.96, 121.79, 119.54, 118.90, 113.98, 111.32, 110.60. HRMS (VTCzNL-Cl, *m*/*z*): $[M]^+$calcd for $C_{42}H_{21}Cl_4N_3$,710.4500; found, 710.6987. Anal. Calcd for $C_{42}H_{21}N_3$: C, 71.11; H, 2.98; N, 5.92. Found: C, 70.98; H, 3.02; N, 5.88.

Synthesis of VTCzNL-Br

First, ICzBF (100 mg, 0.36 mmol), 3,6-dibromo-9*H*-carbazole (232 mg, 0.72 mmol), and Cs_2CO_3 (352 mg, 1.08 mmol) were dissolved in DMAC (20 ml) at room temperature. The mixture was stirred at 170 °Cfor 8 h. After cooling to room temperature, the reaction mixture was poured into a large amount of water. The product was extracted with dichloromethane and the combined organic layers were dried with anhydrous $MgSO_4$. Then, the crude product was evaporated and recrystallized to obtain the white solid VTCzNL-Cl. (170 mg, yield: 54%). ^{1}H NMR (500 MHz, Chloroform-*d*) δ 8.30 (d, J = 1.9 Hz, 4H), 8.01 (d, J = 8.0 Hz, 2H), 7.72 (s, 1H), 7.59 (td, J = 7.8, 1.1 Hz, 2H), 7.50 (d, J = 1.9 Hz, 2H), 7.49 (d, J = 1.9 Hz, 2H), 7.31 (s, 2H), 7.29 (s, 2H), 7.16 (t, J = 7.7 Hz, 2H), 7.01–6.90 (m, 2H). ^{13}C NMR (126 MHz, Chloroform-d) δ 138.62, 138.32, 128.81, 128.79, 126.93, 126.42, 124.38,123.40, 122.61, 121.85, 118.88, 114.04, 112.94, 111.36, 111.00. HRMS (VTCzNL-Br, *m*/*z*): $[M]^+$calcd for $C_{42}H_{21}Br_4N_3$,888.2700; found, 890.0790. Anal. Calcd for $C_{42}H_{21}N_3$: C, 56.86; H, 2.39; N, 4.74. Found: C, 56.69; H, 2.44; N, 4.85.

Data availability

All data generated or analyzed during this study are included in this published article and its ESI† files. Additional datasets used and/or analyzed during the current study are available from the corresponding author on reasonable request.

Author contributions

X. Z., L. L., X. X. and X.-F. L. conceived and designed the project. T.-M. Li, S. N., J.-Y. W., X. Z. and L. L. performed the experiments. X. X. and X.-F. L. drafted and finished the manuscript. All authors have discussed the results and given approval to the manuscript.

Conflicts of interest

There are no conflicts to declare.

Acknowledgements

T.-M. Li and L.-Y. Hu contributed equally to this work. This work was supported by the Key Project of Biomedicine Joint Fund of Hebei Natural Science Foundation (B2020208043) and Hebei innovation center of pharmaceutical and chemical engineering (225676121H).

Notes and references

1 M. Baroncini, G. Bergamini and P. Ceroni, *Chem. Commun.*, 2017, **53**, 2081.
2 A. De, C. M. Perez, A. Liang, K. Wang, L. Dou, O. Prezhdo and L. Huang, *J. Am. Chem. Soc.*, 2024, **146**, 4260.
3 R. Matsuoka, S. Kimura, T. Miura, T. Ikoma and T. Kusamoto, *J. Am. Chem. Soc.*, 2023, **145**, 13615.
4 D. Lee, O. Bolton, B. C. Kim, J. H. Youk, S. Takayama and J. Kim, *J. Am. Chem. Soc.*, 2013, **135**, 6325.
5 Y. Tani, M. Komura and T. Ogawa, *Chem. Commun.*, 2020, **56**, 6810.
6 A. Haque, K. M. Alenezi, M. S. Khan, W.-Y. Wong and P. R. Raithby, *Chem. Soc. Rev.*, 2023, **52**, 454.
7 X. F. Luo, H. B. Han, Z. P. Yan, Z. G. Wu, J. Su, J. W. Zou, Z. Q. Zhu, Y. X. Zheng and J. L. Zuo, *ACS Appl. Mater. Interfaces*, 2020, **12**, 23172.

8 S. Garain, S. M. Wagalgave, A. A. Kongasseri, B. C. Garain, S. N. Ansari, G. Sardar, D. Kabra, S. K. Pati and S. J. George, *J. Am. Chem. Soc.*, 2022, **144**, 10854.
9 K. Chen, Y. Luo, M. Sun, C. Liu, M. Jia, C. Fu, X. Shen, C. Li, X. Zheng, X. Pu, Y. Huang and Z. Lu, *Angew. Chem., Int. Ed.*, 2024, **63**, e202314447.
10 X. Yang, G. I. N. Waterhouse, S. Lu and J. Yu, *Chem. Soc. Rev.*, 2023, **52**, 8005.
11 N. A. Kukhta and C. K. Luscombe, *Chem. Commun.*, 2022, **58**, 6982.
12 X. F. Luo, H. X. Ni, H. L. Ma, Z. Z. Qu, J. Wang, Y. X. Zheng and J. L. Zuo, *Adv. Opt. Mater.*, 2022, **10**, 2102513.
13 W. Feng, D. Chen, Y. Zhao, B. Mu, H. Yan and M. Barboiu, *J. Am. Chem. Soc.*, 2024, **146**, 2484.
14 Q. Zhou, T. Yang, Z. Zhong, F. Kausar, Z. Wang, Y. Zhang and W. Z. Yuan, *Chem. Sci.*, 2020, **11**, 2926.
15 J. Li, Y. Wu and X. Gong, *Chem. Sci.*, 2023, **14**, 3705.
16 S. K. Bhaumik, S. K. Panda and S. Banerjee, *Chem. Commun.*, 2023, **59**, 10396.
17 Y. Takeda, P. Data and S. Minakata, *Chem. Commun.*, 2020, **56**, 8884.
18 R. Gao, M. S. Kodaimati and D. Yan, *Chem. Soc. Rev.*, 2021, **50**, 5564.
19 S. K. Mellerup and S. Wang, *Chem. Soc. Rev.*, 2019, **48**, 3537.
20 W.-L. Zhou, W. Lin, Y. Chen and Y. Liu, *Chem. Sci.*, 2022, **13**, 7976.
21 P. Pattanayak, A. Nandi and P. Purkayastha, *Chem. Mater.*, 2023, **35**(22), 9799.
22 B. T. Phelan, M. W. Mara and L. X. Chen, *Chem. Commun.*, 2021, **57**, 11904.
23 X.-F. Luo, H.-X. Ni, L. Shen, L. Wang, X. Xiao and Y.-X. Zheng, *Chem. Commun.*, 2023, **59**, 2489.
24 J. Cui, S. H. Ali, Z. Shen, W. Xu, J. Liu, P. Li, Y. Li, L. Chen and B. Wang, *Chem. Sci.*, 2024, **15**, 4171.
25 D. Liang, J.-H. Jia, X.-B. Cai, Y.-Q. Zhao, Z.-Q. Wang and C.-Z. Lu, *Inorg. Chem. Front.*, 2022, **9**, 6561.
26 X.-F. Luo, X. Xiao and Y.-X. Zheng, *Chem. Commun.*, 2024, **60**, 1089.
27 M. Du, M. Mai, D. Zhang, L. Duan and Y. Zhang, *Chem. Sci.*, 2024, **15**, 3148.
28 I. Bhattacharjee, N. Acharya and D. Ray, *Chem. Commun.*, 2019, **55**, 1899.
29 P. Palanisamy, O. P. Kumar, H. U. Kim, K. R. Naveen, J.-Y. Kim, J.-H. Baek, M. Y. Chae and J. H. Kwon, *Chem. Eng. J.*, 2024, **481**, 148781.
30 X.-F. Luo, S.-Q. Song, X. Wu, C.-F. Yip, S. Cai and Y.-X. Zheng, *Aggregate*, 2023, **4**, e445.
31 A. M. Polgara and Z. M. Hudson, *Chem. Commun.*, 2021, **57**, 10675.
32 J. Feng, Y.-J. Zhang, S.-H. Ma, C. Yang, Z.-P. Wang, S.-Y. Ding, Y. Li and W. Wang, *J. Am. Chem. Soc.*, 2022, **144**, 6594.
33 Y. Tian and G. Zhu, *Chem. Rev.*, 2020, **120**, 8934.
34 P. Wu and X.-P. Yan, *Chem. Soc. Rev.*, 2013, **42**, 5489.
35 X.-F. Luo, S.-Q. Song, H.-X. Ni, H. Ma, D. Yang, D. Ma, Y.-X. Zheng and J.-L. Zuo, *Angew. Chem., Int. Ed.*, 2022, **61**, e202209984.
36 H. Bhatia, S. Dey and D. Ray, *ACS Omega*, 2021, **6**, 3858.
37 X. Tang, L. Tu, X. Zhao, J. Chen, Y. Ning, F. Wu and Z. Xiong, *J. Phys. Chem. C*, 2022, **126**, 9456.
38 Z. Gu, W. Ma, J. Feng, Z. Liu, B. Xu and W. Tian, *J. Phys. Chem. Lett.*, 2023, **14**, 6437.
39 R. Zhang and J. Yuan, *Acc. Chem. Res.*, 2020, **53**, 1316.